The Journal of Immunology

Molecular Basis of the Functional Differences between Soluble Human Versus Murine MD-2: Role of Val^{135} in Transfer of Lipopolysaccharide from CD14 to MD-2

Jozica Vasl, Alja Oblak, Tina T. Peternelj, Javier Klett, Sonsoles Martín-Santamaría, Theresa L. Gioannini, Jerrold P. Weiss and Roman Jerala

J Immunol published online 29 January 2016
http://www.jimmunol.org/content/early/2016/01/29/jimmunol.1502074

The Journal of Immunology is published twice each month by The American Association of Immunologists, Inc., 9650 Rockville Pike, Bethesda, MD 20814-3994.

Print ISSN: 0022-1767 Online ISSN: 1550-6606.

Published January 29, 2016, doi:10.4049/jimmunol.1502074

Molecular Basis of the Functional Differences between Soluble Human Versus Murine MD-2: Role of Val^{135} in Transfer of Lipopolysaccharide from CD14 to MD-2

Jožica Vašl,* Alja Oblak,* Tina T. Peternelj,* Javier Klett,† Sonsoles Martín-Santamaría,† Theresa L. Gioannini,‡,§,[1] Jerrold P. Weiss,‡ and Roman Jerala*,¶

Myeloid differentiation factor 2 (MD-2) is an extracellular protein, associated with the ectodomain of TLR4, that plays a critical role in the recognition of bacterial LPS. Despite high overall structural and functional similarity, human (h) and murine (m) MD-2 exhibit several species-related differences. hMD-2 is capable of binding LPS in the absence of TLR4, whereas mMD-2 supports LPS responsiveness only when mMD-2 and mTLR4 are coexpressed in the same cell. Previously, charged residues at the edge of the LPS binding pocket have been attributed to this difference. In this study, site-directed mutagenesis was used to explore the hydrophobic residues within the MD-2 binding pocket as the source of functional differences between hMD-2 and mMD-2. Whereas decreased hydrophobicity of residues 61 and 63 in the hMD-2 binding pocket retained the characteristics of wild-type hMD-2, a relatively minor change of valine to alanine at position 135 completely abolished the binding of LPS to the hMD-2 mutant. The mutant, however, retained the LPS binding in complex with TLR4 and also cell activation, resulting in a murine-like phenotype. These results were supported by the molecular dynamics simulation. We propose that the residue at position 135 of MD-2 governs the dynamics of the binding pocket and its ability to accommodate lipid A, which is allosterically affected by bound TLR4. ***The Journal of Immunology*****, 2016, 196: 000–000.**

Endotoxins (e.g., LPS), which are the main components of the Gram-negative bacterial cell envelope, are able to activate the innate immune system at picomolar concentrations, leading to the release of proinflammatory cytokines, such as TNF-α, IL-1, IL-6, and IL-8 (1, 2). Recognition of the LPS is a complex process where transmembrane protein TLR4, myeloid differentiation factor 2 (MD-2), and CD14 play crucial roles (3). CD14 binds and accumulates LPS and presents it to the TLR4/MD-2 receptor complex, which, by dimerization, delivers a signal through the plasma membrane. It is essential that glycoprotein MD-2 binds to both LPS and the extracellular domain of TLR4 ($TLR4_{ecd}$). MD-2 presents the exposed acyl chain of the hexaacylated lipid A moiety of LPS to $TLR4_{ecd}$, which triggers receptor dimerization. $TLR4_{ecd}$ adopts a horseshoe-like shape consisting of leucine-rich repeats (4), whereas MD-2 is characterized by a β-cup fold structure composed of two antiparallel β-sheets forming a large hydrophobic pocket for ligand binding (5–7). Several crystal structures of MD-2 from different species and with different bound ligands, including agonists and antagonists, have been determined (6–8). In these structures, the four acyl chains of the lipid IVa fit into the MD-2 pocket. The sixth acyl chain of LPS remains at the surface of MD-2, partially exposed to the solvent, and forms a hydrophobic interface for the TLR4 from the neighboring TLR4/MD-2/LPS complex, triggering the receptor dimerization and activation. Despite the proposed global structural changes upon binding of agonist or antagonist, the crystal structure of the TLR4/MD-2/LPS complex (9) and molecular studies of the MD-2 hydrophobic loop (10) demonstrated that the size of the MD-2 pocket remains unchanged and the structural changes are localized to the edge of the pocket.

Although there is a high degree of structural similarity, MD-2 orthologs exhibit some important functional differences, including the binding of certain endotoxin chemotypes (hypoacylated lipid A) and mimetics (paclitaxel), or the ability of these ligands to act as TLR4 agonists (11, 12). Notably, murine (m) and human (h) MD-2 differ in their discrimination between lipid A (506) and lipid IVa (406) (13, 14). Mutagenesis studies revealed that several residues in the hydrophobic pocket of mMD-2 (e.g., 42, 57, 61, and 69) and residues at the entrance of the hydrophobic pocket (e.g., 122 and 125) influence the agonist activity of lipid IVa (13, 15). It has been further shown that residues 82 and 122 of MD-2 govern species-specific activation of TLR4 by tetra- and pentaacylated endotoxins (16). Finally, there is an apparent functional difference between the two species: hMD-2, but not mMD-2, is

*Department of Biotechnology, National Institute of Chemistry, 1000 Ljubljana, Slovenia; †Center for Biological Research, Superior Council for Scientific Research, 28040 Madrid, Spain; ‡Inflammation Program, Department of Microbiology, Carver College of Medicine, University of Iowa, Iowa City, IA 52241; §Veterans Affairs Medical Center, Iowa City, IA 52246; and ¶Excellent Nuclear Magnetic Resonance–Future Innovation for Sustainable Technologies Center of Excellence, 1000 Ljubljana, Slovenia

[1]Deceased.

ORCIDs: 0000-0001-8495-6568 (J.K.); 0000-0002-7679-0155 (S.M.-S.); 0000-0003-1476-4485 (J.P.W.).

Received for publication September 21, 2015. Accepted for publication December 26, 2015.

This work was supported by Slovenian Research Agency Grants J1-9795, J1-2271, and P4-0176, a bilateral Slovenian–United States collaborative grant, National Institute of Allergy and Infectious Diseases Grant AI05732 (to J.P.W.), and by grants from the Veterans Administration (to T.L.G.). This work was also supported by Spanish Ministry of Economy and Competitiveness Grants CTQ2011-22724 and CTQ2014-57141-R and by European Commission Grant H2020-MSC-ETN-642157 (TOLLerant project).

Address correspondence and reprint requests to Prof. Roman Jerala, Department of Biotechnology, National Institute of Chemistry, Hajdrihova 19, P.O. Box 660, SI-1000 Ljubljana, Slovenia. E-mail address: roman.jerala@ki.si

Abbreviations used in this article: e, equine; h, human; HEK, human embryonic kidney; HSA, human serum albumin; LBP, LPS-binding protein; LOS, lipooligosaccharide; m, murine; MD, molecular dynamics; MD-2, myeloid differentiation factor; NMR, nuclear magnetic resonance; ps, picosecond; s, soluble; SASA, solvent-accessible surface area; TBSTT, TBS (pH 7.5) containing 0.05% Tween 20 and 0.2% Triton X-100; $TLR4_{ecd}$, TLR4 extracellular domain; wt, wild-type.

able to react with LPS when expressed and secreted in the absence of TLR4 to ultimately form a functional complex with TLR4 (17–20).

Our study aimed to identify the residues of hMD-2 required for the ligand binding to soluble MD-2 (sMD-2). Several residues in the hydrophobic pocket of hMD-2 have been replaced with the corresponding mMD-2 residues or with the residues with modified hydrophobicity. Most residues in the hydrophobic pocket of MD-2 are conserved. The residues at positions 61 and 63 that are occupied by hydrophobic residues did not cause any differences. Surprisingly, however, the residue at position 135 exhibited a large effect, although it lies at the very bottom of the pocket. Replacement of Val^{135} by Ala, as in mouse MD-2, inactivated the ability of MD-2 to bind LPS while maintaining its ability to bind and activate cells when present in the complex with TLR4. This indicates that the residue at position 135 is important for the function of MD-2. We propose, based on the experimental results and a molecular dynamics (MD) simulation, that this residue plays a role in the dynamics of the MD-2 binding pocket, with an allosteric effect of the bound TLR4.

Materials and Methods

Cell culture and reagents

Human embryonic kidney (HEK) 293 cells were provided by Dr. J. Chow (Eisai Research Institute, Andover, MA). HEK293 cells stably transfected with TLR4 (HEK293/TLR4 no. BF1) were provided by Dr. Douglas Golenbock (University of Massachusetts Medical Center, Worcester, MA) and Dr. Andra Schromm (Research Center Borstel, Borstel, Germany). HEK293T cells, used for the analysis of complex formation between lipooligosaccharide (LOS) and MD-2 using gel filtration chromatography and in immunoblotting experiments, were provided by Dr. Fabio Re (University of Tennessee Health Sciences Center, Memphis, TN). Expression plasmids containing the sequences of human TLR4 and MD-2 as well as the pELAM-1 firefly luciferase plasmid were a gift from Dr. C. Kirschning (Institute of Medical Microbiology, University of Duisburg–Essen, Essen, Germany). Expression plasmid containing the sequence of mouse TLR4 was purchased from InvivoGen (San Diego, CA). Expression plasmid for mouse MD-2 was a gift from Dr. Y. Nagai (University of Tokyo, Tokyo, Japan). The *Renilla* luciferase phRL-TK plasmid was purchased from Promega (Fitchburg, WI). The nucleotide sequences encoding MD-2 were cloned into pEF-BOS vector with Flag and His tags on the C-terminal. The nucleotide sequences encoding TLR4 were cloned into pUNO vector with C-terminal HA tag. Transfection reagent JetPEI was purchased from Polyplus-Transfection (Illkirch, France) and was used according to the manufacturer's instructions. S-LPS (from *Salmonella abortus equi* HL83) was purchased from Sigma-Aldrich (St. Louis, MO). *Escherichia coli*–type lipid A (compound 506) was obtained from the Peptide Institute (Osaka, Japan). Purified [^{3}H]LOS (25,000 cpm/pmol) was isolated from an acetate auxotroph of *Neisseria meningitidis* serogroup B after metabolic labeling, as described (21). Sephacryl S500 and S200 HR size exclusion gel matrices were purchased from GE Healthcare (Buckinghamshire, U.K.). Human serum albumin (HSA) was obtained as an endotoxin-free, 25% stock solution (Baxter Health Care, Deerfield, IL). Anti–Tetra-His Abs and goat anti-mouse HRP-conjugated secondary Abs were from Qiagen (Valencia, CA) and Jackson Immunologicals (West Grove, PA), respectively. LPS-binding protein (LBP) and sCD14 were gifts from XOMA (Berkeley, CA) and Amgen (Thousand Oaks, CA), respectively. An AlphaLISA IL-8 immunoassay research kit was acquired from PerkinElmer (Waltham, MA).

Site-directed mutagenesis

All mutations were introduced into pEFBOS-h or -m MD-2-FLAG-His plasmid using a QuikChange site-directed mutagenesis kit (Stratagene, La Jolla, CA) according to the manufacturer's instructions. All plasmids were sequenced to confirm the mutation. Primer sequences will be made available upon request.

Preparation of [^{3}H]LOS$_{agg}$ and [^{3}H]LOS:sCD14 complex

[^{3}H]LOS$_{agg}$ and the [^{3}H]LOS:sCD14 complex were prepared as previously described (22–24). Briefly, [^{3}H]LOS$_{agg}$ (M_r of $>20 \times 10^6$) were obtained after hot phenol extraction of [^{3}H]LOS followed by ethanol precipitation of [^{3}H]LOS$_{agg}$ and ultracentrifugation. Monomeric [^{3}H]LOS:CD14 complexes (M_r of ~60,000) were prepared by treatment of [^{3}H]LOS$_{agg}$ for 30 min at 37°C with a substoichiometric LBP (molar ratio LOS/LBP, 100:1) and 1- to 1.5-fold molar excess sCD14 followed by gel exclusion chromatography (Sephacryl S200, 1.6 × 70-cm column) in PBS (pH 7.4), 0.03% HSA to isolate monomeric [^{3}H]LOS:sCD14 complex. Radiochemical purity of [^{3}H]LOS$_{agg}$ and [^{3}H]LOS:sCD14 was confirmed by Sephacryl S500 (LOS$_{agg}$) or S200 ([^{3}H]LOS:sCD14) chromatography (21, 24).

Production and reaction of sMD-2 and sMD-2/TLR4$_{ecd}$ with [^{3}H]LOS:sCD14

HEK293T cells were plated in a six-well plate with 10% FBS in DMEM. Cells were transfected the following day with an expression plasmid encoding MD-2 alone (wild-type [wt] or mutant) or cotransfected with expression plasmids encoding MD-2 and TLR4$_{ecd}$ using PolyFect reagent (Qiagen), as previously described (25). After 12–16 h, the medium was replaced with 1.5 ml serum-free medium (DMEM) plus 0.1% HSA. The medium was spiked with [^{3}H]LOS:sCD14 (1 nM) at the time of medium replacement to permit the reaction of [^{3}H]LOS:sCD14 with the newly secreted MD-2 with and without wt TLR4$_{ecd}$. The reaction products were analyzed by Sephacryl HR S200 (1.6 × 30 cm) chromatography in PBS. Fractions (0.5 ml) were collected at a flow rate of 0.5 ml/min at room temperature using ÄKTApurifier or ÄKTAexplorer 100 fast protein liquid chromatography (GE Healthcare). Radioactivity in collected fractions was analyzed by liquid scintillation spectroscopy (Beckman LS liquid scintillation counter). In all cases, the recovery rate of [^{3}H]LOS was ≥70%. All the solutions used were pyrogen free and sterile filtered.

HEK293 cell activation assays: Dual-Luciferase reporter assay and AlphaLISA assay

HEK293 cells were seeded into 96-well plates (Costar, Corning, NY) with 10% FBS in DMEM, at 3×10^4 cells/well, and incubated overnight in a humidified atmosphere (5% CO_2) at 37°C. The next morning, cells were cotransfected for 4 h with pEFBOS- (wt or mutant, human or murine) MD-2-FLAG-His and pUNO- (human or murine) TLR4-HA together with NF-κB–dependent luciferase and constitutive *Renilla* reporter plasmids using Lipofectamine 2000 (Invitrogen Life Technologies Waltham, MA). After 4 h, medium was removed and replaced with DMEM plus 10% FBS. The following day, cells were incubated with S-LPS for 16 h, as indicated. In selected experiments, HEK293 cells were seeded into 96-well plates (3×10^4 cells/well) and separately transfected either with mMD-2 (wt or mutant) or with TLR4 (human or murine) together with NF-κB–dependent luciferase and constitutive *Renilla* reporter plasmids. After 16 h, aliquots of the conditioned medium of HEK293 cells containing sMD-2 were added to HEK293 TLR4 cells where the supernatants have been removed. The cells were then activated with lipid A for 16 h. In a different approach, HEK293 cells were seeded into 12-well plates (3×10^5 cells/well) and transfected either with mMD-2 (wt or mutant) or with TLR4 (human or murine) together with NF-κB–dependent luciferase and constitutive *Renilla* reporter plasmids. After 16 h, the cells were resuspended in fresh medium containing 10% serum, joined in 1:1 ratio, and reseeded together in 96-well plates to yield cocultures of cells separately expressing MD-2 or TLR4. The following day, the cells were incubated in the presence of S-LPS or lipid A for 16 h. After the activation with S-LPS or lipid A, the supernatants were harvested and the cells were lysed in 1× reporter assay lysis buffer (Promega) and analyzed for reporter gene activities using a Dual-Luciferase reporter assay system on a Mithras LB940 luminometer. Relative luciferase activity was calculated by normalizing each sample's luciferase activity for constitutive *Renilla* activity measured within the same sample. When plotting data the value of the unstimulated sample with wt hMD-2 was set to 1 and other values were adjusted accordingly. In the supernatants of HEK293 cells, IL-8 concentrations were determined with an AlphaLISA IL-8 immunoassay research kit (PerkinElmer), according to the manufacturer's instructions.

Immunoblotting

To detect polyhistidine-labeled wt and mutant MD-2, an anti-polyhistidine Ab (Tetra-His Ab, Qiagen) was used. We expressed wt MD-2 and MD-2 mutants in HEK293T cells, which do not express MD-2 without transfection with expression plasmids encoding MD-2 (11, 18). HEK293T cells were transiently transfected with wt or mutant MD-2 using PolyFect (Qiagen) as a transfection reagent. The medium was changed 12 h after transfection and replaced with serum-free medium. Aliquots of conditioned medium from transfected and mock-transfected HEK293T cells were harvested after 24 h. Equal volumes of the medium and Laemmli sample buffer containing DTT were combined, and each sample was electrophoresed (Bio-Rad mini gel system) through a 4–15% gradient acrylamide gel (Tris/HEPES/SDS buffer) and transferred to nitrocellulose membrane. The membrane was washed with TBS (pH 7.5) containing 0.05% Tween 20 and 0.2% Triton X-100 (TBSTT),

blocked to reduce nonspecific background with 5% dried nonfat milk in TBSTT for 1 h at 25˚C, and incubated with the anti-His[4] Ab in the blocking solution overnight. After washing with TBSTT, the blot was incubated with goat anti-mouse IgG conjugated to HRP for 1 h at 25˚C in the blocking solution and washed extensively with TBSTT. Blots were developed using the Pierce SuperSignal substrate system. By reducing immunoblot samples, each MD-2 species was converted to the monomeric form, migrating as a triplet (hMD-2) or quadruplet (mMD-2) due to the differences in glycosylation (26). Recovered extracellular media (supernatants) were immunoblotted to confirm that levels of expression of wt and mutant MD-2 were comparable.

Computational methods

Preparation of the macromolecules and myristic acids. The three-dimensional coordinates of human and mouse MD-2 proteins were obtained from the corresponding x-ray crystallographic structure. Mutation of Val^{135} to Ala was done with PyMOL mutation wizard (http://www.pymol.org) in all studied systems. Caps to the N-terminal and C-terminal residues were added, ligands (when present) and crystallographic water molecules were deleted, missing hydrogens were added, and protonation state of ionizable groups was computed by using Maestro protein preparation wizard version 9.3 (Schrödinger, New York, NY). Atom types and charges were assigned according to AMBER ff10 force field (27). Each resulting system was immersed in a rectangular box of explicit TIP3P water molecules (28) extending 10 Å away from any protein atom for simulating the aqueous environment with the help of AmberTools 13 (University of California San Francisco, San Francisco, CA). Coordinates for myristic acids were extracted from PDB 2e56, and parameters from gaff BCC force field were used. Myristate ionization state was considered for the calculations.

MD simulations. MD simulations were run with Amber 12 (University of California San Francisco). Before the MD simulations, all hydrated systems were equilibrated under the following protocol: initial 8000 steps of steepest descent minimization, followed by heating of the system with position restrain (force constant of 20 kcal mol^{-1} $Å^{-2}$) for all protein atoms with MD simulation increasing the temperature from 100 to 300˚C during 10 picoseconds (ps) and additional 15 ps at constant 300˚C. Position restrain was gradually decreased during 100 ps at constant 300˚C, until the full system was under no restrains with constant temperature and pressure. After equilibration, 50 ns MD simulation was run for all systems at constant temperature (300˚C) and pressure (1 atm). Short- and long-range forces were calculated every one and two time steps, respectively (each time step = 2.0 fs), constraining the covalent bonds involving hydrogen atoms to their equilibrium values. Long-range electrostatic interactions were accounted for using the particle mesh Ewald approach (29), applying periodic boundary conditions. The root mean square deviation as a function of time with respect to the starting structure for the α-C atoms was computed for all the studied systems showing main changes in the first 5 ns and complete convergence beyond 10 ns until the end of simulation.

Average structures. With the help of the ptraj module of AmberTools 13, for each MD simulation of the eight systems, five average structures were extracted corresponding to the following time slots: from 0 to 2.5 ns (AVG-1), from 2.5 to 5 ns (AVG-2), from 5 to 10 ns (AVG-3), from 10 to 20 ns (AVG-4), and from 20 to 50 ns (AVG-5). All average structures were minimized with 5000 steps of steepest descent minimization with position restrain (force constant of 10 kcal mol^{-1} $Å^{-2}$) for all nonhydrogen atoms, plus 5000 steps of steepest descent minimization with no restrains.

Solvent-accessible surface area and volume calculations. Solvent-accessible surface area (SASA) and solvent-accessible volume were calculated on hydrophobic pockets of MD-2 by using the CASTp server (30). The CASTp server identifies and computes the molecular area and volume for cavities and pockets of a given protein. In our case, we computed SASA and volumes of the hydrophobic pocket of MD-2 for the 40 structures corresponding to the five average structures derived from each studied molecular system.

Results

Mutations in the hydrophobic pocket of hMD-2 do not affect hMD-2 expression and TLR4 activation

MD-2 has a narrow and deep binding pocket with hydrophobic residues lining the internal surface and positively charged residues located at the opening rim of the cavity (6, 7). This pocket accommodates acyl chains of the lipid A. To study the role of hydrophobic amino acids in the binding pocket of hMD-2, we prepared point mutations at positions

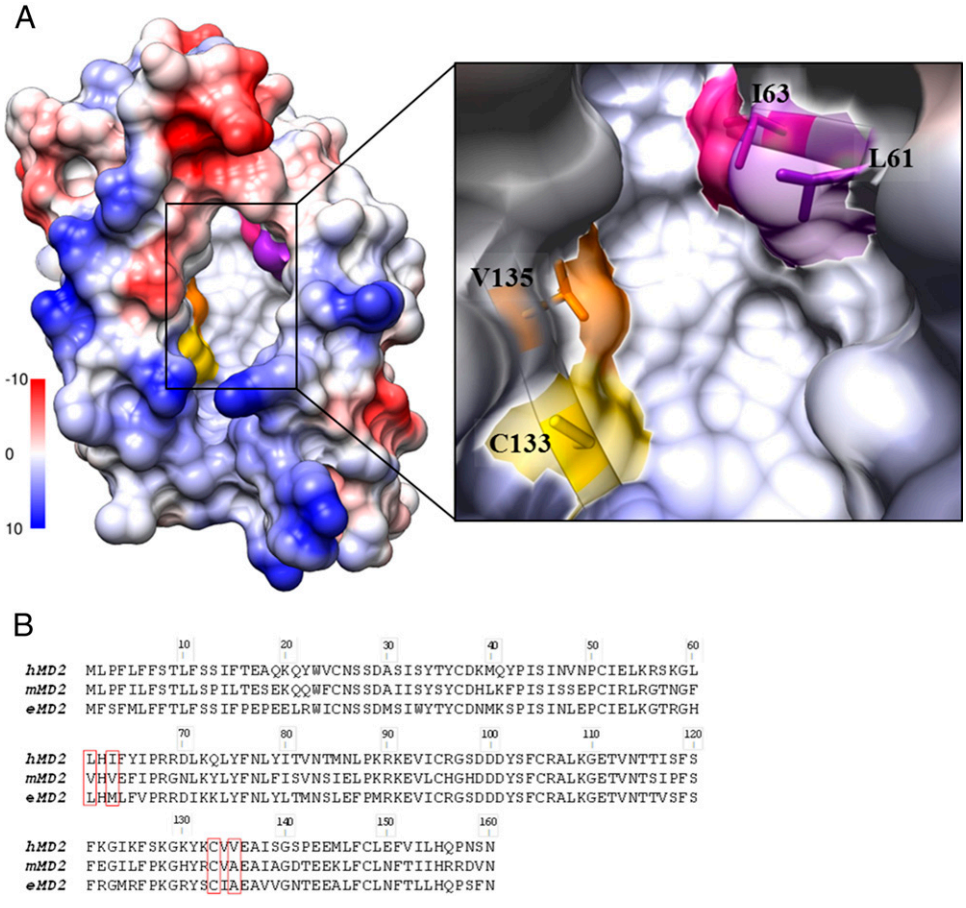

FIGURE 1. The hydrophobic pocket of human MD-2. (**A**) *Left*, An electrostatic surface representation of hMD-2 (Protein Data Bank ID 2E56) (Coulombic coloring), showing the hydrophobic pocket (white surface). *Right*, A close-up of the hydrophobic pocket with amino acid residues L61, I63, C133, and V135 shown in purple, pink, yellow, and orange, respectively. (**B**) Amino acid alignment of human, murine, and equine MD-2.

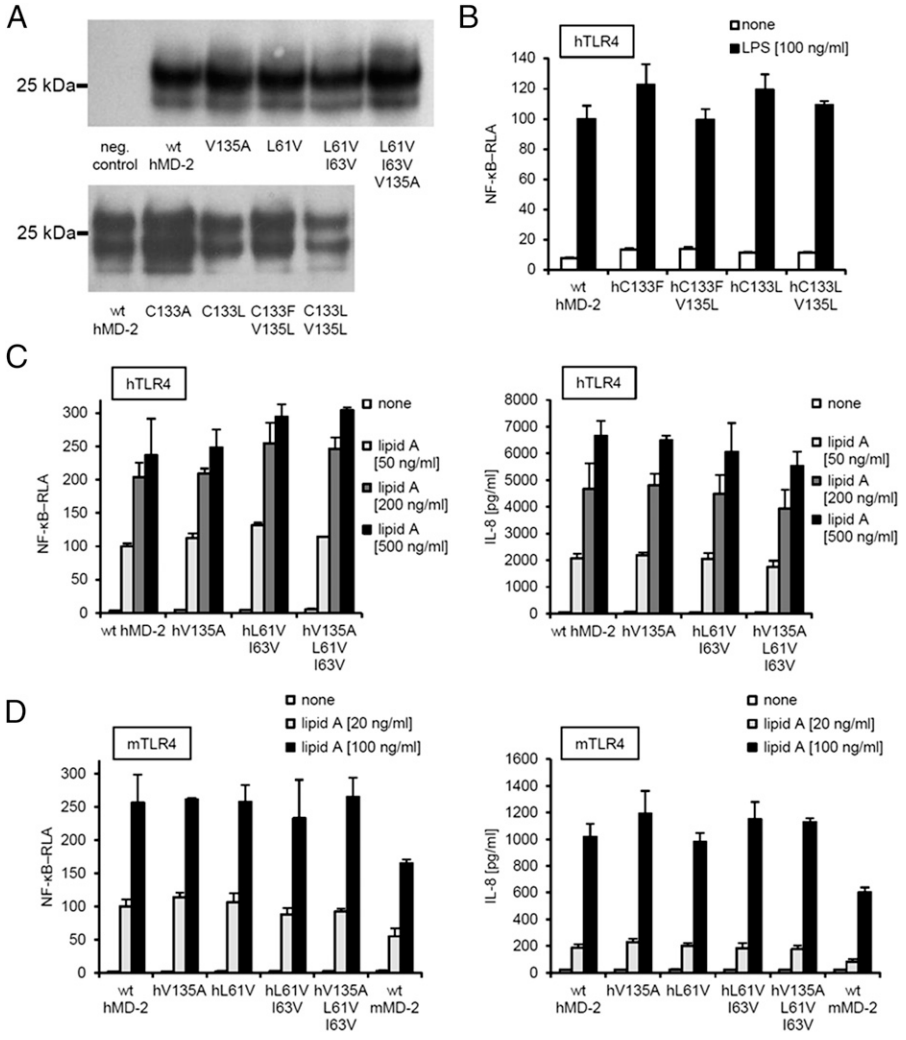

FIGURE 2. Effect of mutations at residues 61, 63, 133, and 135 of hMD-2. (**A**) Secretion of mutants into the medium from HEK293T cells transfected with expression plasmids encoding wt hMD-2 or mutant hMD-2. Multiple bands reflect differences in MD-2 glycosylation. (**B**–**D**) NF-κB–dependent reporter activity or IL-8 production of lipid A–stimulated HEK293 cells transfected with hMD-2 with replaced residues at positions 61, 63, 133, and 135, with residues with increased (C133F, C133L, C133F V135L, C133L V135L) or decreased (V135A, L61V, L61V I63V, L61V I63V V135A) hydrophobicity. HEK293 cells were transiently transfected with expression plasmids encoding MD-2 together with hTLR4 or mTLR4 and reporter luciferase plasmids. Results are representative of two or more experiments.

within the hydrophobic binding pocket where human and mouse MD-2 differ, namely residues Leu[61], Ile[63], and Val[135] (Fig. 1A). Hydrophobic residues are conserved at these positions; however, the size and hydrophobicity of the residues might underlie the species–specific differences. To test this hypothesis, residues 61, 63, and 135 of hMD-2 were replaced with the corresponding mMD-2 residues, each smaller and less hydrophobic than their hMD-2 counterparts. Next, additional mutants of hMD-2 with more hydrophobic residues at positions Cys[133] and Val[135] were tested. Finally, two mMD-2 mutants with corresponding hMD-2 residues were prepared and evaluated (A135V and A135V E122K).

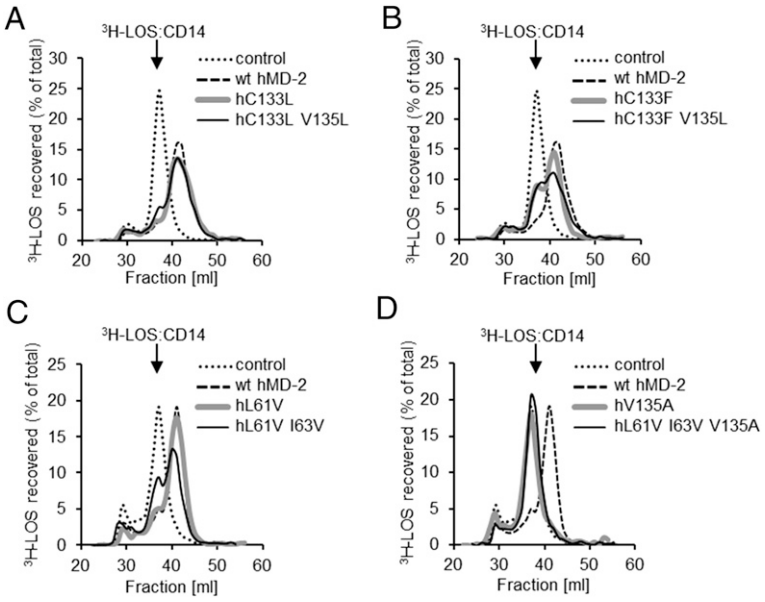

FIGURE 3. The effect of changes in hydrophobicity of amino acid residues at 61, 63, 133, and 135 of hMD-2 on the ability of sMD-2 to react with [³H]LOS:sCD14 and form monomeric [³H]LOS:MD-2 complex. Shown are mutants of hMD-2 with increased hydrophobicity at residues Cys[133] and Val[135] (**A** and **B**), less hydrophobic single or double mutants at Leu[61] and Ile[63] (**C**), and mutation of a single residue, Val[135], to Ala (**D**). Soluble MD-2 (wt or mutant) was produced using transiently transfected HEK293T cells and tested for the ability to bind LOS (i.e., transfer LOS from the [³H]LOS:CD14 complex) using Sephacryl S200 chromatography as described in *Materials and Methods*. Note that the peaks of elution of [³H]LOS:sCD14 and [³H]LOS:MD-2 were at 37 and 42 ml, respectively. The results shown are from one experiment, representative of at least two independent determinations.

We first examined the effects of these mutations on the expression and secretion of MD-2. The cell lysates and extracellular media from transiently transfected HEK293T cells expressing either wt hMD-2 or hMD-2 mutants were analyzed by immunoblotting. Fig. 2A shows that all hMD-2 mutants were expressed and secreted at a similar level as for wt hMD-2. This facilitated the interspecies comparison of the hMD-2 ability to promote cellular response to endotoxin. Fig. 2B–D demonstrate that none of the mutations affected hMD-2 coreceptor functional activity, as assessed by the ability of hMD-2 to support LPS-induced TLR4 activation when coexpressed in cells with hTLR4 or mTLR4.

Effect of mutations in the hydrophobic pocket of hMD-2 on LPS binding

To investigate the effect of mutations in the hydrophobic pocket of hMD-2 on endotoxin binding, we initially assayed the transfer of added radiolabeled monomeric [^{3}H]LOS:sCD14 to soluble wt and mutant MD-2 that were expressed and secreted by transiently transfected HEK293T cells. MD-2 requires presentation of LOS/LPS as part of a monomeric LOS(LPS):protein complex with CD14 for high-affinity (pM) binding of endotoxin. Transfer of [^{3}H]LOS from CD14 (M_r of ~60,000) to sMD-2 (M_r of ~25,000) was monitored by size exclusion chromatography, as previously described (24). Although all the mutants preserved the competence of wt hMD-2 to support LPS-triggered TLR4 activation (Fig. 2B–D), not all the mutant proteins retained the ability to bind [^{3}H]LOS:sCD14 and form monomeric [^{3}H]LOS:MD-2 complex (Fig. 3). Mutants with increased hydrophobicity at residues Cys^{133} (C133F) and Val^{135} (V135L) were found to bind LOS and form the LOS:MD-2 monomer at the same elution volume as the wt hMD-2 (Fig. 3A, 3B). Furthermore, less hydrophobic single or double mutants at Leu^{61} and Ile^{63} of hMD-2 (L61V, L61V I63V) also exhibited LPS binding similar to wt hMD-2, as shown by reactivity with LOS:sCD14 (Fig. 3C), and supported normal (wt hMD-2) TLR4-dependent cell activation by endotoxin (Fig. 2C, 2D). In contrast, mutation of a single residue, Val^{135} to Ala, completely abolished the transfer of [^{3}H]LOS from [^{3}H]LOS:sCD14 to the MD-2 mutant (Fig. 3D). However, there were no changes in the functional activities of hMD-2 V135A and L61V I63V V135A

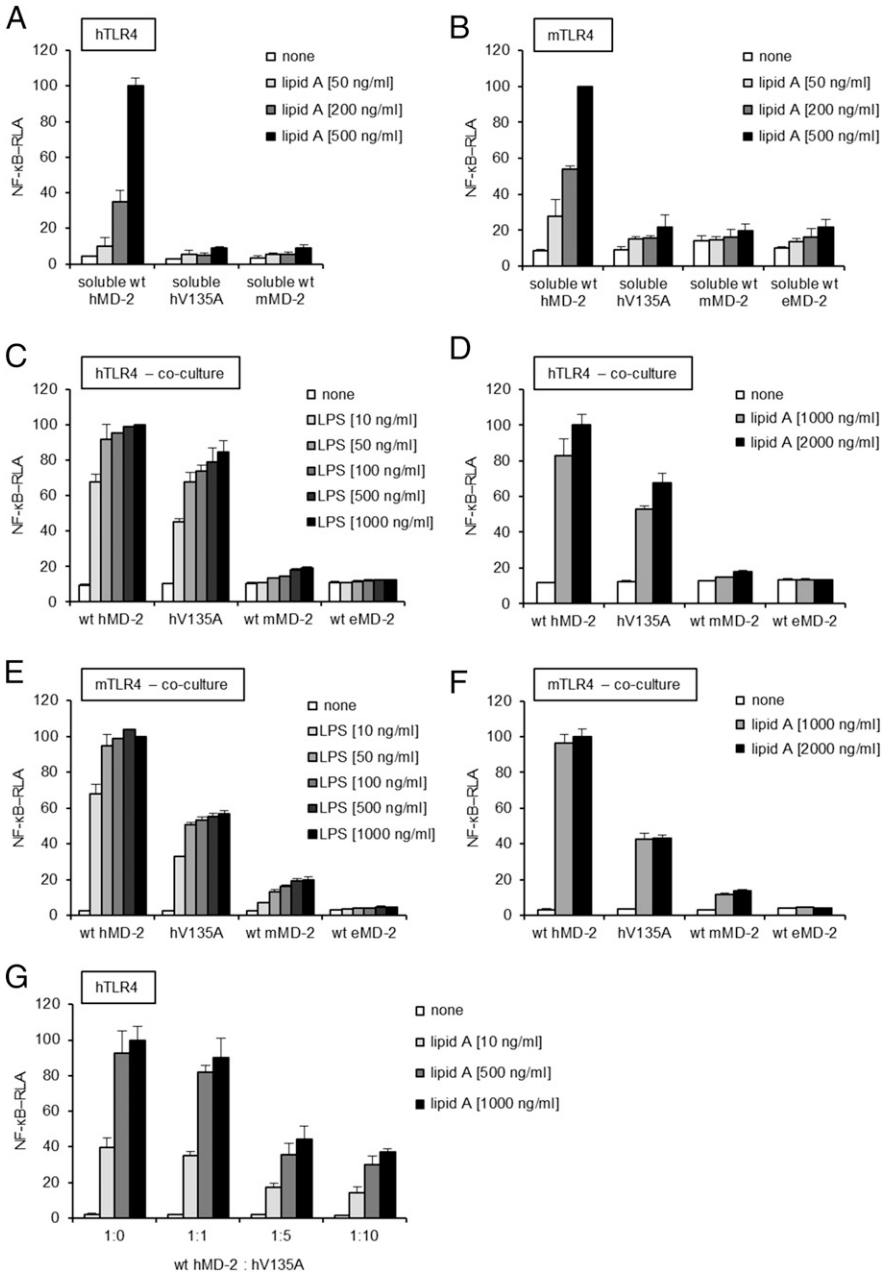

FIGURE 4. Cell activation by LPS, mediated by MD-2 variants via soluble proteins or cell coculture. (**A** and **B**) HEK293 cells were transiently transfected with plasmids encoding MD-2. After 24 h, harvested medium containing sMD-2 was incubated with lipid A (50, 200, or 500 ng/ml) and added to HEK293 cells that had been transfected with a plasmid encoding hTLR4 or mTLR4 together with NF-κB–dependent luciferase reporter plasmid. (**C**–**F**) Coculture of HEK293 cells transfected with plasmids encoding wt or V135A hMD-2 and cells transfected with TLR4 and NF-κB–dependent luciferase reporter plasmids. Cocultured cells were stimulated with increasing concentration of S-LPS or lipid A for 16 h. (**G**) Inhibition of TLR4 signaling with soluble V135A hMD-2. Culture medium of HEK293 cells transfected with plasmids encoding wt hMD-2 together with V135A hMD-2, in ratios from 1:0 to 1:10, was incubated with lipid A (10, 500, or 1000 ng/ml) and then added to HEK293 cells that had been transfected with a plasmid encoding hTLR4 together with NF-κB–dependent luciferase reporter plasmid. All results shown are means ± SEM relative luciferase activity (RLA) from three independent experiments.

variants, as measured by luciferase reporter assay or AlphaLISA assay performed in HEK293/TLR4 cells (Fig. 2C, 2D).

Activity of soluble V135A hMD-2 is strongly reduced in comparison with soluble wt hMD-2

LPS can activate human cells through binding to hMD-2 that is already associated with TLR4$_{ecd}$ or through binding of the hMD-2/LPS complex to the ectodomain of TLR4 (22, 24, 31). Murine MD-2 differs from its human ortholog, as it does not form a detectable mMD-2/LPS complex (17, 20). The inability of secreted V135A hMD-2 to react with [^{3}H]LOS:sCD14 suggested that this mutant may have impaired ability to support LPS-induced activation in the cells expressing TLR4 without MD-2 and whose LPS sensing ability depends on the addition of soluble MD-2. To test this hypothesis, we compared the ability of secreted (soluble) wt hMD-2 and V135A hMD-2 to confer activation of HEK293/TLR4 cells by LPS. As shown in Fig. 4A and 4B, cells transfected with either hTLR4 or mTLR4 were unable to respond to LPS in the presence of a medium containing soluble V135A hMD-2. This coincided with the differences observed in the reaction of V135A hMD-2 with [^{3}H]LOS:sCD14 (Fig. 3D). It has been reported that MD-2 is secreted as a labile molecule that, during a relatively short period of time, may lose its biological activity at physiological temperature in a serum-free medium (32). When, however, freshly synthesized soluble hMD-2 is exposed to LPS and CD14, it converts to a stable MD-2/LPS complex that is capable of activating TLR4 (24, 33–35). Because the presence of LPS significantly stabilized MD-2, we therefore performed the similar experiment by spiking the cell medium with LPS so that all secreted MD-2 could immediately bind LPS and increase its stability. However, relative to the wt hMD-2, the biological activity of V135A mutant was reduced to the same extent as when LPS was added subsequently (Fig. 4A, 4B). Most MD-2 orthologs have a valine residue at position 135, with notable exceptions of murine and horse (equine [e]) MD-2 that have alanine at this position. Consequently, we predicted that isolated eMD-2, similar to mMD-2, would not be able to bind LPS in solution. Indeed, soluble eMD-2 did not confer activation of HEK293/mTLR4 cells by LPS (Fig. 4B) however, cotransfection of hTLR4 or mTLR4 with eMD-2 resulted in LPS-triggered activation (16). Alternatively, coculture of cells secreting MD-2 variants and cells expressing TLR4 and luciferase reporter demonstrated only slightly lower response by the mutated V135A hMD-2 (Fig. 4C and 4D and Fig. 4E and 4F for hTLR4 and mTLR4, respectively). This suggests that the secreted V135A MD-2 mutant is functional, yet it loses the competence to mediate LPS signaling unless it is rapidly recruited to TLR4.

Next, we assessed whether soluble V135A hMD-2 mutant, apart from failing to bind endotoxin, also lacks the ability to bind TLR4, which would be expected if the mutation affects the global protein fold. For this purpose, TLR4-expressing HEK293 cells were incubated with a constant amount of soluble wt hMD-2 and increasing amounts of soluble V135A hMD-2. As indicated in Fig. 4G, soluble biologically inactive V135A hMD-2 caused a dose-dependent inhibition of TLR4 activation that was otherwise induced by the added wt hMD-2 plus lipid A. This result is most compatible with a selective deficiency in LPS (but not TLR4) binding, resulting at higher doses in a reduced fraction of TLR4 available to bind wt hMD-2 and respond to the added lipid A.

LPS binding to soluble hMD-2 coexpressed with TLR4$_{ecd}$

Previous research has shown that the TLR4 ectodomain can rescue the functional activity (i.e., LPS binding) of MD-2 variants prone to aggregation by stabilizing the functional, monomeric state of MD-2 (10, 25, 36, 37). In our study, the retained functional responsiveness to LPS of the cells coexpressing TLR4 and V135A hMD-2 (Fig. 2D) indicated that preassociation of V135A hMD-2 with the TLR4 ectodomain might sustain the interaction of V135A hMD-2 with [^{3}H]LOS:sCD14, as compared with secreted V135A hMD-2 in the absence of TLR4. To test this hypothesis, experiments were repeated with cells coexpressing wt hMD-2 or V135A hMD-2 with hTLR4$_{ecd}$. As shown in Fig. 5, the addition of [^{3}H]LOS:sCD14 to the culture medium of the cells expressing wt hMD-2 and hTLR4$_{ecd}$ resulted in a nearly complete conversion of [^{3}H]LOS:sCD14 to the earlier eluting (M_r of ~190,000) and later eluting (M_r of ~25,000) [^{3}H]LOS-containing complexes representing ([^{3}H]LOS:MD-2:TLR4$_{ecd}$)$_2$ (37) and [^{3}H]LOS:MD-2 (35), respectively. As predicted, coexpression of V135A hMD-2 with hTLR4$_{ecd}$ resulted in a transition of [^{3}H]LOS:sCD14 to ([^{3}H]LOS: V135A MD-2:TLR4$_{ecd}$)$_2$ but not to [^{3}H]LOS: V135A MD-2 (Fig. 5). This demonstrates that the association of V135A hMD-2 with TLR4$_{ecd}$ is prerequisite for the reaction of V135A hMD-2 with [^{3}H]LOS:sCD14. V135A hMD-2 fails to bind LPS in the absence of TLR4 (Figs. 3, 5), and TLR4 activation is achieved only when V135A hMD-2 and TLR4 are expressed in the same cell (Fig. 2C, 2D) or by the neighboring cells (Fig. 4C–F).

The reverse mMD-2 A135V mutant confirms the role of Val^{135} in soluble hMD-2 to bind endotoxin

The above findings indicate that the ability of wt hMD-2 to form bioactive soluble MD-2 can be completely abolished by a single substitution of valine 135 with alanine that is present in wt mMD-2. To test the role of Ala^{135} for the inability of mMD-2 to form bioactive sMD-2 when expressed in the absence of TLR4, residue

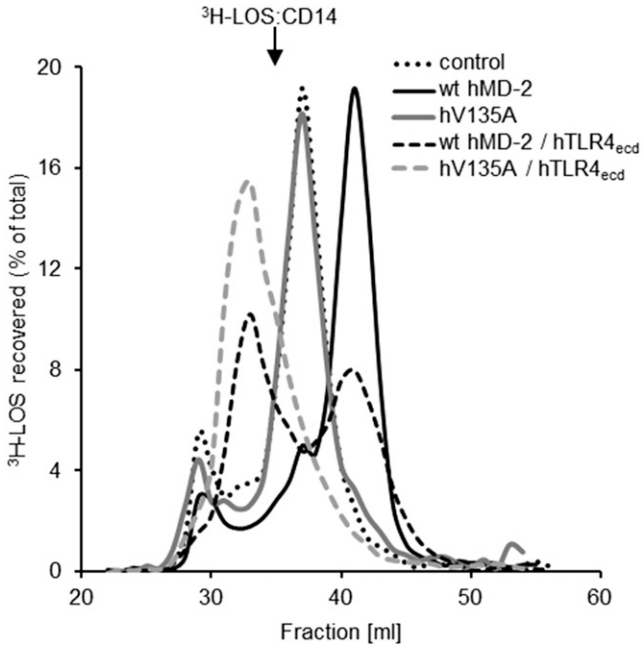

FIGURE 5. Binding of [^{3}H]LOS:sCD14 to V135A hMD-2 in the presence of TLR4$_{ecd}$. HEK293T cells were cotransfected with plasmids encoding hTLR4$_{ecd}$ and wt or mutant hMD-2, as indicated. After 24 h, the transfection medium was changed with serum-free medium and spiked with 1 nM [^{3}H]LOS:sCD14. Medium was harvested at 24 h and analyzed by Sephacryl S500 size exclusion chromatography. Resolved reactants and products were monitored by liquid scintillation spectroscopy. Note that the reaction of [^{3}H]LOS:sCD14 with MD-2:TLR4$_{ecd}$ yields ([^{3}H]LOS:MD-2/TLR4$_{ecd}$)$_2$ complex, whereas the interaction of [^{3}H]LOS:sCD14 with sMD-2 leads to the formation of [^{3}H]LOS:MD-2. The results shown are representative of two or more experiments.

135 in mMD-2 was replaced with valine, as the corresponding amino acid present in wt hMD-2 (A135V). Wild-type mMD-2 is secreted in a much lower amount in comparison with wt hMD-2 (20) (Fig. 6A). Although recovery of secreted mMD-2 was not measurably improved by the single A135V mutation (Fig. 6A), increased TLR4 activation by lipid A was observed, especially in the cells expressing mTLR4 and cocultured with cells expressing and secreting A135V mMD-2 (Fig. 6B–E). Combination of the A135V mutation with a mutation (E122K) that alone markedly increases secretion of mMD-2 without conferring functional reactivity and responses to LPS (20) yielded a much greater recovery of the secreted MD-2 (Fig. 6A) and greater TLR4 responsiveness to lipid A (Fig. 6B–E). These findings demonstrate that the Ala^{135} residue of mMD-2 contributes to the restriction of its biological activity in the soluble form.

MD simulations of WT and V135A mutant TLR4/MD-2 systems: computational studies of the binding pocket collapse

To obtain a molecular insight of the putative conformational changes in the ligand-free MD-2 prior to LPS binding, MD simulations were performed with MD-2 or TLR4/MD-2 systems in aqueous solvent without lipids, as these structures represent an obligatory intermediate step before the binding of LPS, and also in complex with three myristic acids, as observed in some x-ray crystallographic structures. Ten molecular systems were built corresponding to hMD-2 protein alone (systems 1–4, wt and mutant, agonist and antagonist conformation), hMD-2 protein in complex with TLR4 (systems 5 and 6, wt and mutant), mMD-2 (systems 7 and 8, agonist and antagonist conformation), and hMD-2 protein in complex with three myristic acids (systems 9 and 10, wt and mutant, antagonist conformation). Systems 1–8, lacking any lipid inside the MD-2 pocket, were submitted to MD simulations in explicit solvent (water) during 50 ns. Changes of the SASA and solvent-accessible volume of the hydrophobic pocket of MD-2 were monitored along the simulation time, as well as conformational changes in different regions of the protein. Wild-type hMD-2 structures were observed to suffer a hydrophobic collapse, accordingly to a quick decrease of the pocket volume and SASA, leading to closed pocket structures (Fig. 7). In the case of mutant hMD-2, and similarly mMD-2, the pocket volume and SASA also decreased at the first stages of the simulation, but stuck at some point in a half-closed pocket, and the full collapse was not observed. This could point to a decreased flexibility of V135A hMD-2 and wt mMD-2. This loss of plasticity could account for a poorer ability to bind LPS in accordance with the biological assays. In the case of hTLR4/MD2 complexes, both systems 5 and 6 (wt and mutant) exhibited similar dynamics, showing high values of pocket volume and SASA along the simulation, with no meaningful differences (Fig. 7B). We observed that the pocket dynamics of MD-2 in complex with the TLR4 ectodomain was significantly reduced.

In wt hMD-2, Val^{135} is surrounded by three phenyl rings from the corresponding Phe^{76}, Phe^{147}, and Phe^{151} residues, and stability of this association can be supported through CH–π interactions between the Val^{135} side chain and the aromatic ring from Phe^{76}. In mMD-2, naturally occurring Ala^{135} is also surrounded by three phenylalanine side chains, with similar spatial disposition. Scrutiny of the conformational change events revealed that, in wt hMD-2, the Phe^{76} and Phe^{147} side chains remarkably change their initial position during the simulations. Phe^{76} orients the phenyl ring toward the Phe^{147} away from Val^{135}. This movement pushes the rotation of Phe^{147} side chain, whereas the Phe^{151} side chain almost maintains its initial crystallographic position. In the mutant and, interestingly, in the mMD-2, the three phenylalanine side chains do not move

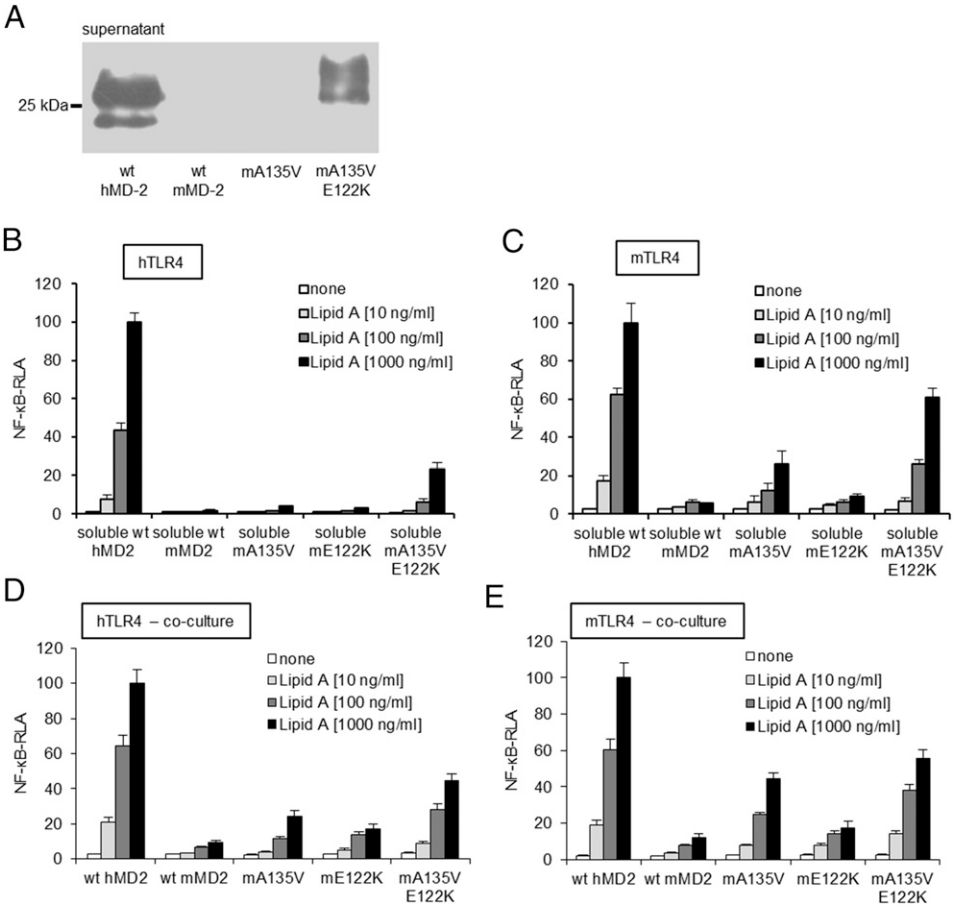

FIGURE 6. The effect of mMD-2 mutations on the ability to activate cells by lipid A. (**A**) Wild-type mMD-2 exhibits drastically lower extracellular accumulation compared with wt hMD-2. E122K substitution induces a substantial increase in secretion and recovery of extracellular mMD-2. (**B** and **C**) Activity of secreted soluble mMD-2 is increased with A135V/E122K double mutation. Medium of HEK293 cells transfected with plasmids encoding MD-2 was added to HEK293 cells transfected with a plasmid encoding hTLR4 or mTLR4 together with NF-κB–dependent luciferase reporter plasmid. Cells were stimulated with lipid A (10, 100, and 1000 ng/ml) and assayed for luciferase activity. (**D** and **E**) Coculture of HEK293 cells transiently transfected with plasmids encoding wt or mutant mMD-2 and HEK293 cells transfected with hTLR4 or mTLR4 and NF-κB–dependent luciferase reporter plasmids. Cocultured cells were stimulated with lipid A (10, 100, and 1000 ng/ml) for 16 h and assayed for luciferase activity. All the results shown are means ± SEM relative luciferase activity (RLA) from three independent experiments.

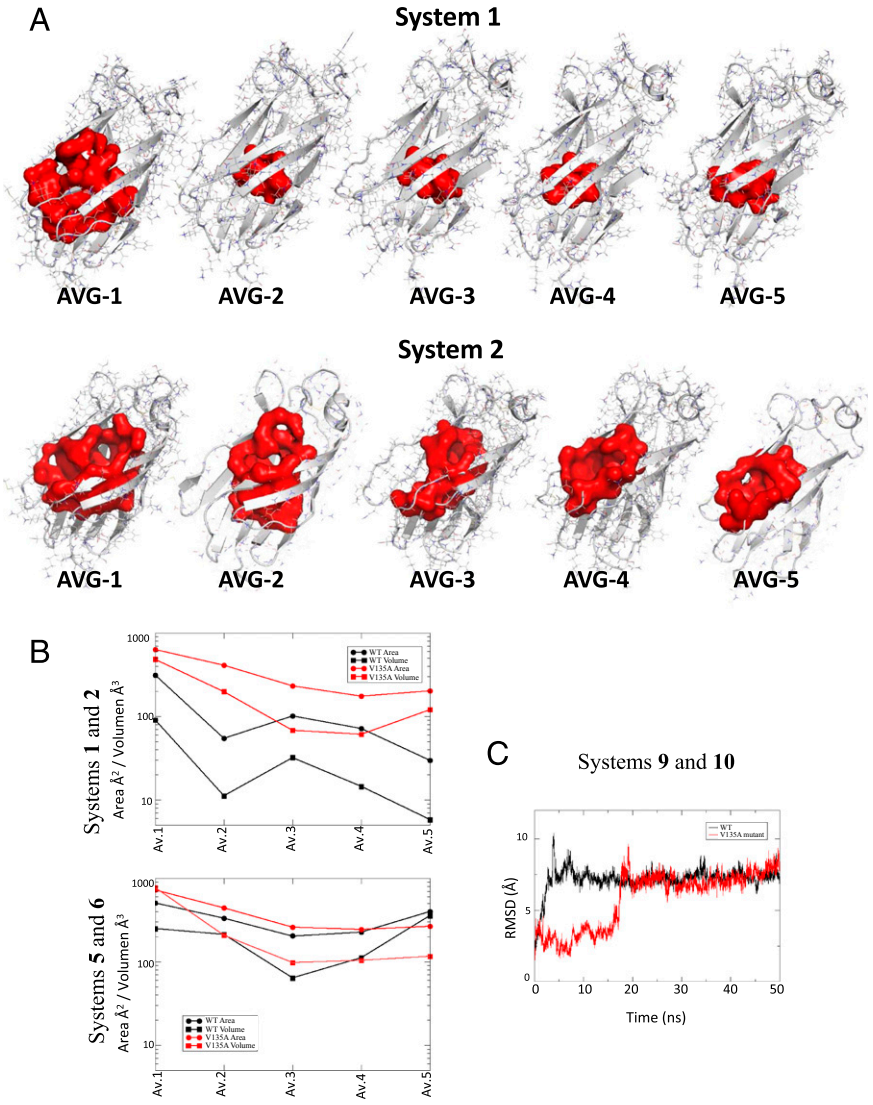

FIGURE 7. MD simulation analysis of free MD-2 and MD-2 bound to TLR4 ectodomain. (**A**) CASTp-calculated volumes of the MD-2 pocket for the molecular systems 1 (wt) and 2 (V135A mutant) corresponding to hMD-2 in the agonist conformation from PDB-ID 3FXI. (**B**) CASTp-calculated SASA and volumes of the MD-2 pocket for the molecular systems 1 and 2 (corresponding to hMD-2 in the agonist conformation from PDB-ID 3FXI) and 5 and 6 (corresponding to hMD-2 in the antagonist conformation from PDB-ID 2E59). (**C**) Variation of the root mean square deviation (RMSD) of the heavy atoms of the three myristic acids with respect to the starting geometry along the 50-ns MD simulation for the complex of wt MD-2 with three myristic acids (system 9, in black) and for the complex of mutant V135A hMD-2 with three myristic acids (system 10, in red). The average structures come from the MD simulations (50 ns, explicit water). Ordinate values are expressed in the logarithm scale. (B and C) Values for the WT and V135A are depicted in black and red, respectively, with area and volume labeled with circles and squares, respectively.

significantly from the starting crystal-derived geometry. This observation seems to point to a lower plasticity of the V135A variant, both the mutant hMD-2 and wt mMD-2. Analysis of the structural changes in the protein–protein interfaces (dimerization and primary interfaces) does not allow us to conclude any consequence for the dimerization event.

MD simulations of the hMD-2 protein in complex with three myristic acids (systems 9 and 10, wt and mutant) led to the observation that the wt type complex (system 9) gains stability much faster along the simulation time, whereas in the case of the complex of the V135A mutant hMD-2 (system 10), the myristic acids are stabilized only after 20 ns of simulation (Fig. 7C). This slower adaptation to the lipids supports the hypothesis of a lower plasticity for the V135A hMD-2 mutant and a decreased ability to accommodate lipidic ligands.

Discussion

The MD-2 protein is profoundly involved in cellular response to endotoxins from Gram-negative bacteria. It is also required for TLR4 signaling in nearly all investigated cases of endogenous sterile inflammation agonists investigated so far (38, 39). Functional differences between human and murine MD-2 have been extensively investigated by the modeling, docking, and point mutations (12, 13, 20, 40). In this study, we focused on the hydrophobic interactions between the acyl chains of LPS and the amino acid residues in the hydrophobic cavity of MD-2. Increasing the hydrophobicity of hMD-2 binding pocket preserved both cellular responsiveness to endotoxin (Fig. 2B) and transfer of endotoxin from CD14 to the MD-2 (Fig. 3A, 3B). Moreover, decreased hydrophobicity of the pocket at Leu[61] and Ile[63] retained the characteristics of wt hMD-2 (Fig. 2C). Surprisingly, a relatively minute change of valine to alanine at position 135 significantly impaired the binding of LPS to soluble MD-2 (Fig. 3D). This led to a hypothesis that Ala[135] impairs the ability of mMD-2 to bind LPS in the absence of TLR4. The striking effect of a single amino acid residue at this position could play a critical role in the cellular response to endotoxins, contributing to the interspecies differences.

An important clue on the ability of alanine residue at position 135 to disable the bioactivity of soluble mMD-2 is provided by the fact that coexpression of mMD-2 with mTLR4 eliminates the need for a valine at this site (Fig. 2D). This finding, along with the location of Val[135] at the bottom of the pocket, indicates that the valine residue is not required for direct interactions of mMD-2 with mTLR4 but rather to preserve the bioactivity of soluble MD-2 secreted in the absence of TLR4. Subsequently, as a soluble extracellular protein, MD-2 can interact with endotoxin, presented by CD14, and/or with TLR4. The increased activity of soluble

mMD-2 A135V in comparison with wt mMD-2 (Fig. 6) confirmed our hypothesis that Val^{135}, either directly or indirectly, preserves the bioactivity of soluble MD-2. In contrast to wt hMD-2, recombinant hMD-2 V135A was unable to bind LPS presented by CD14 or activate TLR4-transfected HEK293 cells. Accordingly, we propose that, despite the small difference in chemical properties between valine in human versus alanine in murine MD-2, valine increases the stability of bioactive MD-2 monomers in the absence of TLR4. Of note, equine MD-2 has alanine at position 135 and it phenocopies murine MD-2 by being biologically inactive when secreted without TLR4 but active when coexpressed with TLR4, further supporting our conclusions/hypothesis.

Both LPS binding (i.e., transfer of LPS monomer from CD14 to MD-2) and TLR4 binding require and stabilize MD-2 monomers (35). Thus, conceivably the effect of the alanine for valine substitution at residue 135 could be on the stability of MD-2 monomers. However, the ability of secreted V135A hMD-2 to competitively inhibit activation of TLR4 by lipid A when added in excess of wt hMD-2 suggests a much more discrete structural effect on MD-2 monomers that selectively affects LPS/lipid A binding. The finding that secreted V135A hMD-2 can partially reconstitute functional MD-2/TLR4 receptors on the neighboring cells expressing TLR4 alone (Fig. 4C–F) indicates that TLR4 binding soon after secretion can rescue the LPS binding function of V135A hMD-2. The inability of later exposure of secreted V135A hMD-2 to TLR4 to reconstitute functional MD-2/TLR4 receptors (Fig. 4A, 4B, 4G) indicates a time-dependent selective loss of LPS binding by MD-2(/TLR4) that cannot be reversed by subsequent association with TLR4 and, hence, not mediated by a more direct role of TLR4 in the binding of LPS to V135A hMD-2/TLR4 heterodimers.

Secreted wt mMD-2 has no detectable functional activity, as assessed either by reactivity with [^{3}H]LOS:sCD14 spiked into the culture medium (20) or via the LPS-triggered activation of HEK293/mTLR4 cells (Fig. 6C). Although single residue substitution E122K in mMD-2 yielded detectable amounts of soluble MD-2 (20), it had no functional activity. However, the substitutions A135V with/without E122K led to a significant increase in the bioactivity of soluble mMD-2 (Fig. 6). Taken together, these findings suggest the contribution of Lys^{122} in enhanced secretion of MD-2 and Val^{135} in maintaining the LPS-binding competence of soluble mMD-2. Molecular mechanism underlying the rescue of the functionality of soluble mMD-2 by association with TLR4 is in part the result of prevented aggregation due to its low solubility. Comparison of the surface charge distribution of MD-2 from different species shows significant differences in the electrostatic potential around the ligand-binding cavity (40). Alternatively, even the soluble mMD-2 mutants with increased net charge were unable to bind LPS, suggesting an additional factor in maintaining the competence for LPS binding. Position of Ala^{135} deep inside the binding pocket could not affect its solubility but rather the binding pocket dynamics. We speculate that the structure of soluble V135A hMD-2 has a higher propensity to collapse in the absence of TLR4 and blunt the cellular signaling. In fact, MD simulations point out the possibility of a collapse of the binding pocket in the absence of bound residential lipids. It is likely that different lipid ligands may bind to MD-2 in the absence of LPS, as the myristates were observed in the crystal structure of human MD-2 (6). Although the simulation of the whole process of the residential lipid dissociation from MD-2 and the kinetics of LPS binding to MD-2 is beyond the current computational ability of the MD simulations, the simulations presented in the present study provide a plausible explanation accounting for a decreased plasticity of the V135A hMD-2 protein, thus leading to a diminished ability to bind host lipids such as myristic acid. We propose as a plausible scenario that the closing of the hydrophobic cavity occurs rapidly upon mMD-2 or V135A hMD-2 mutant secretion from the cell in the absence of TLR4. This collapsed conformation resembles the structure of the MD-2 homolog Der p 2 (41). The structure of Der p 2 has been investigated by both nuclear magnetic resonance (NMR) (42) and x-ray crystallography (41). An overlay of the two Der p 2 structures indicated significant flexibility of the protein structure. The β-sheets in the Der p 2 x-ray structure are significantly farther apart than in the NMR model and create an internal cavity, which is occupied by hydrophobic ligand, whereas the NMR structure displays a collapsed binding pocket. Hence, we propose the existence of two MD-2 modes, closed and opened, depending on the cellular environment (i.e., presence of TLR4, LPS, other lipids). We suggest that soluble mMD-2 has a propensity for a closed, biologically inactive mode in the absence of bound TLR4 ectodomain and lower concentrations of surrounding host lipids, whereas soluble hMD-2, due to the Val^{135}, has a higher population of an opened mode, ready to bind the lipid-like ligands regardless of the presence of TLR4. This hypothesis might be confirmed by a high resolution structure of soluble mMD-2, because only the TLR4-bound (stabilized) structure of mMD-2 has been determined so far (43).

In conclusion, results of this study provide to the best of our knowledge the first evidence for the role of specific hydrophobic residues that are responsible for the competence of the circulating MD-2 for binding of LPS in the absence of TLR4, allowing LPS responsiveness of cells that do not express MD-2. The different MD-2 orthologs presented in this study (hMD-2, mMD-2, eMD-2) suggest that subtle differences in molecular structure can have significant influence on the signaling process. Excessive production of inflammatory mediators may be harmful to host tissue, and hence MD-2 represents an attractive therapeutic target of inflammatory and immune diseases. Our findings thus provide important information on the hydrophobic LPS binding site that may support development of potential therapeutic agents.

Disclosures

The authors have no financial conflicts of interest.

References

1. Rossol, M., H. Heine, U. Meusch, D. Quandt, C. Klein, M. J. Sweet, and S. Hauschildt. 2011. LPS-induced cytokine production in human monocytes and macrophages. *Crit. Rev. Immunol.* 31: 379–446.
2. Verhasselt, V., C. Buelens, F. Willems, D. De Groote, N. Haeffner-Cavaillon, and M. Goldman. 1997. Bacterial lipopolysaccharide stimulates the production of cytokines and the expression of costimulatory molecules by human peripheral blood dendritic cells: evidence for a soluble CD14-dependent pathway. *J. Immunol.* 158: 2919–2925.
3. Jerala, R. 2007. Structural biology of the LPS recognition. *Int. J. Med. Microbiol.* 297: 353–363.
4. Bella, J., K. L. Hindle, P. A. McEwan, and S. C. Lovell. 2008. The leucine-rich repeat structure. *Cell. Mol. Life Sci.* 65: 2307–2333.
5. Gruber, A., M. Mancek, H. Wagner, C. J. Kirschning, and R. Jerala. 2004. Structural model of MD-2 and functional role of its basic amino acid clusters involved in cellular lipopolysaccharide recognition. *J. Biol. Chem.* 279: 28475–28482.
6. Ohto, U., K. Fukase, K. Miyake, and Y. Satow. 2007. Crystal structures of human MD-2 and its complex with antiendotoxic lipid IVa. *Science* 316: 1632–1634.
7. Kim, H. M., B. S. Park, J.-I. Kim, S. E. Kim, J. Lee, S. C. Oh, P. Enkhbayar, N. Matsushima, H. Lee, O. J. Yoo, and J.-O. Lee. 2007. Crystal structure of the TLR4-MD-2 complex with bound endotoxin antagonist Eritoran. *Cell* 130: 906–917.
8. Jin, M. S., and J.-O. Lee. 2008. Structures of the Toll-like receptor family and its ligand complexes. *Immunity* 29: 182–191.
9. Park, B. S., D. H. Song, H. M. Kim, B.-S. Choi, H. Lee, and J.-O. Lee. 2009. The structural basis of lipopolysaccharide recognition by the TLR4-MD-2 complex. *Nature* 458: 1191–1195.
10. Resman, N., J. Vasl, A. Oblak, P. Pristovsek, T. L. Gioannini, J. P. Weiss, and R. Jerala. 2009. Essential roles of hydrophobic residues in both MD-2 and Toll-like receptor 4 in activation by endotoxin. *J. Biol. Chem.* 284: 15052–15060.
11. Kawasaki, K., S. Akashi, R. Shimazu, T. Yoshida, K. Miyake, and M. Nishijima. 2000. Mouse toll-like receptor 4.MD-2 complex mediates lipopolysaccharide-mimetic signal transduction by Taxol. *J. Biol. Chem.* 275: 2251–2254.

12. Resman, N., H. Gradisar, J. Vasl, M. M. Keber, P. Pristovsek, and R. Jerala. 2008. Taxanes inhibit human TLR4 signaling by binding to MD-2. *FEBS Lett.* 582: 3929–3934.
13. Muroi, M., and K. Tanamoto. 2006. Structural regions of MD-2 that determine the agonist-antagonist activity of lipid IVa. *J. Biol. Chem.* 281: 5484–5491.
14. Meng, J., E. Lien, and D. T. Golenbock. 2010. MD-2-mediated ionic interactions between lipid A and TLR4 are essential for receptor activation. *J. Biol. Chem.* 285: 8695–8702.
15. Meng, J., J. R. Drolet, B. G. Monks, and D. T. Golenbock. 2010. MD-2 residues tyrosine 42, arginine 69, aspartic acid 122, and leucine 125 provide species specificity for lipid IVA. *J. Biol. Chem.* 285: 27935–27943.
16. Oblak, A., and R. Jerala. 2014. Species-specific activation of TLR4 by hypoacylated endotoxins governed by residues 82 and 122 of MD-2. *PLoS One* 9: e107520.
17. Visintin, A., K. A. Halmen, N. Khan, B. G. Monks, D. T. Golenbock, and E. Lien. 2006. MD-2 expression is not required for cell surface targeting of Toll-like receptor 4 (TLR4). *J. Leukoc. Biol.* 80: 1584–1592.
18. Hajjar, A. M., R. K. Ernst, J. H. Tsai, C. B. Wilson, and S. I. Miller. 2002. Human Toll-like receptor 4 recognizes host-specific LPS modifications. *Nat. Immunol.* 3: 354–359.
19. Fujimoto, T., S. Yamazaki, A. Eto-Kimura, K. Takeshige, and T. Muta. 2004. The amino-terminal region of toll-like receptor 4 is essential for binding to MD-2 and receptor translocation to the cell surface. *J. Biol. Chem.* 279: 47431–47437.
20. Vasl, J., A. Oblak, T. L. Gioannini, J. P. Weiss, and R. Jerala. 2009. Novel roles of lysines 122, 125, and 58 in functional differences between human and murine MD-2. *J. Immunol.* 183: 5138–5145.
21. Giardina, P. C., T. Gioannini, B. A. Buscher, A. Zaleski, D. S. Zheng, L. Stoll, A. Teghanemt, M. A. Apicella, and J. Weiss. 2001. Construction of acetate auxotrophs of *Neisseria meningitidis* to study host-meningococcal endotoxin interactions. *J. Biol. Chem.* 276: 5883–5891.
22. Gioannini, T. L., A. Teghanemt, D. Zhang, E. N. Levis, and J. P. Weiss. 2005. Monomeric endotoxin:protein complexes are essential for TLR4-dependent cell activation. *J. Endotoxin Res.* 11: 117–123.
23. Gioannini, T. L., D. Zhang, A. Teghanemt, and J. P. Weiss. 2002. An essential role for albumin in the interaction of endotoxin with lipopolysaccharide-binding protein and sCD14 and resultant cell activation. *J. Biol. Chem.* 277: 47818–47825.
24. Gioannini, T. L., A. Teghanemt, D. Zhang, N. P. Coussens, W. Dockstader, S. Ramaswamy, and J. P. Weiss. 2004. Isolation of an endotoxin-MD-2 complex that produces Toll-like receptor 4-dependent cell activation at picomolar concentrations. *Proc. Natl. Acad. Sci. USA* 101: 4186–4191.
25. Vasl, J., P. Prohinar, T. L. Gioannini, J. P. Weiss, and R. Jerala. 2008. Functional activity of MD-2 polymorphic variant is significantly different in soluble and TLR4-bound forms: decreased endotoxin binding by G56R MD-2 and its rescue by TLR4 ectodomain. *J. Immunol.* 180: 6107–6115.
26. Wright, S. D., R. A. Ramos, P. S. Tobias, R. J. Ulevitch, and J. C. Mathison. 1990. CD14, a receptor for complexes of lipopolysaccharide (LPS) and LPS binding protein. *Science* 249: 1431–1433.
27. Wang, J., and P. A. Kollman. 2001. Automatic parameterization of force field by systematic search and genetic algorithms. *J. Comput. Chem.* 22: 1219–1228.
28. Jorgensen, W. L., J. Chandrasekhar, J. D. Madura, R. W. Impey, and M. L. Klein. 1983. Comparison of simple potential functions for simulating liquid water. *J. Chem. Phys.* 79: 926.
29. Darden, T., D. York, and L. Pedersen. 1993. Particle mesh Ewald: an $N\cdot\log(N)$ method for Ewald sums in large systems. *J. Chem. Phys.* 98: 10089.
30. Liang, J., H. Edelsbrunner, and C. Woodward. 1998. Anatomy of protein pockets and cavities: measurement of binding site geometry and implications for ligand design. *Protein Sci.* 7: 1884–1897.
31. Gioannini, T. L., A. Teghanemt, D. Zhang, G. Esparza, L. Yu, and J. Weiss. 2014. Purified monomeric ligand.MD-2 complexes reveal molecular and structural requirements for activation and antagonism of TLR4 by Gram-negative bacterial endotoxins. *Immunol. Res.* 59: 3–11.
32. Kennedy, M. N., G. E. D. Mullen, C. A. Leifer, C. Lee, A. Mazzoni, K. N. Dileepan, and D. M. Segal. 2004. A complex of soluble MD-2 and lipopolysaccharide serves as an activating ligand for Toll-like receptor 4. *J. Biol. Chem.* 279: 34698–34704.
33. Schromm, A. B., E. Lien, P. Henneke, J. C. Chow, A. Yoshimura, H. Heine, E. Latz, B. G. Monks, D. A. Schwartz, K. Miyake, and D. T. Golenbock. 2001. Molecular genetic analysis of an endotoxin nonresponder mutant cell line: a point mutation in a conserved region of MD-2 abolishes endotoxin-induced signaling. *J. Exp. Med.* 194: 79–88.
34. Teghanemt, A., P. Prohinar, T. L. Gioannini, and J. P. Weiss. 2007. Transfer of monomeric endotoxin from MD-2 to CD14: characterization and functional consequences. *J. Biol. Chem.* 282: 36250–36256.
35. Teghanemt, A., F. Re, P. Prohinar, R. Widstrom, T. L. Gioannini, and J. P. Weiss. 2008. Novel roles in human MD-2 of phenylalanines 121 and 126 and tyrosine 131 in activation of Toll-like receptor 4 by endotoxin. *J. Biol. Chem.* 283: 1257–1266.
36. Mitsuzawa, H., C. Nishitani, N. Hyakushima, T. Shimizu, H. Sano, N. Matsushima, K. Fukase, and Y. Kuroki. 2006. Recombinant soluble forms of extracellular TLR4 domain and MD-2 inhibit lipopolysaccharide binding on cell surface and dampen lipopolysaccharide-induced pulmonary inflammation in mice. *J. Immunol.* 177: 8133–8139.
37. Prohinar, P., F. Re, R. Widstrom, D. Zhang, A. Teghanemt, J. P. Weiss, and T. L. Gioannini. 2007. Specific high affinity interactions of monomeric endotoxin.protein complexes with Toll-like receptor 4 ectodomain. *J. Biol. Chem.* 282: 1010–1017.
38. Manček-Keber, M., and R. Jerala. 2015. Postulates for validating TLR4 agonists. *Eur. J. Immunol.* 45: 356–370.
39. Manček-Keber, M., M. Frank-Bertoncelj, I. Hafner-Bratkovič, A. Smole, M. Zorko, N. Pirher, S. Hayer, V. Kralj-Iglič, B. Rozman, N. Ilc, et al. 2015. Toll-like receptor 4 senses oxidative stress mediated by the oxidation of phospholipids in extracellular vesicles. *Sci. Signal.* 8: ra60.
40. Walsh, C., M. Gangloff, T. Monie, T. Smyth, B. Wei, T. J. McKinley, D. Maskell, N. Gay, and C. Bryant. 2008. Elucidation of the MD-2/TLR4 interface required for signaling by lipid IVa. *J. Immunol.* 181: 1245–1254.
41. Derewenda, U., J. Li, Z. Derewenda, Z. Dauter, G. A. Mueller, G. S. Rule, and D. C. Benjamin. 2002. The crystal structure of a major dust mite allergen Der p 2, and its biological implications. *J. Mol. Biol.* 318: 189–197.
42. Mueller, G. A., D. C. Benjamin, and G. S. Rule. 1998. Tertiary structure of the major house dust mite allergen Der p 2: sequential and structural homologies. *Biochemistry* 37: 12707–12714.
43. Ohto, U., K. Fukase, K. Miyake, and T. Shimizu. 2012. Structural basis of species-specific endotoxin sensing by innate immune receptor TLR4/MD-2. *Proc. Natl. Acad. Sci. USA* 109: 7421–7426.